



OPEN

Valerian and valeric acid inhibit growth of breast cancer cells possibly by mediating epigenetic modifications

Fengqin Shi^{1,2}, Ya Li^{1,2}, Rui Han^{1,2}, Alan Fu¹, Ronghua Wang^{1,2}, Olivia Nusbaum¹, Qin Qin¹, Xinyi Chen², Li Hou^{1,2} & Yong Zhu¹✉

Valerian root (*Valeriana officinalis*) is a popular and widely available herbal supplement used to treat sleeping disorders and insomnia. The herb's ability to ameliorate sleep dysfunction may signify an unexplored anti-tumorigenic effect due to the connection between circadian factors and tumorigenesis. Of particular interest are the structural similarities shared between valeric acid, valerian's active chemical ingredient, and certain histone deacetylase (HDAC) inhibitors, which imply that valerian may play a role in epigenetic gene regulation. In this study, we tested the hypothesis that the circadian-related herb valerian can inhibit breast cancer cell growth and explored epigenetic changes associated with valeric acid treatment. Our results showed that aqueous valerian extract reduced growth of breast cancer cells. In addition, treatment of valeric acid was associated with decreased breast cancer cell proliferation, migration, colony formation and 3D formation in vitro in a dose- and time-dependent manner, as well as reduced HDAC activity and a global DNA hypomethylation. Overall, these findings demonstrate that valeric acid can decrease the breast cancer cell proliferation possibly by mediating epigenetic modifications such as the inhibition of histone deacetylases and alterations of DNA methylation. This study highlights a potential utility of valeric acid as a novel HDAC inhibitor and a therapeutic agent in the treatment of breast cancer.

Natural products provide a rich source for the development of novel drugs with anti-tumor activities. Currently, over a half of the available anticancer drugs were derived from botanical sources¹. For example, Taxol (paclitaxel) is an FDA approved anti-microtubule agent extracted from bark of the Pacific yew tree *Taxus brevifolia* and has shown a strong anticancer effect in human cancer². Considering herbal extracts and their bioactive compounds are a rich source of therapeutics to human beings, there is a compelling reason to seek novel bioactive compounds in the herbal extracts.

Valerian root is an herb that has long been found to be effective for treating circadian related sleep disorders. The name "Valerian" in Latin means "to be strong or healthy", which can be attributed to its use as an herbal remedy that has been in practice since ancient Greek and Roman times. Currently, the herb is used mainly as a treatment for insomnia and is considered among the most popular sleeping aids in Europe³. Valerian has been approved as a Generally Recognized as Safe (GRAS) food ingredient by the U.S. Food and Drug Administration (FDA). A recent systematic review of research concluded that "The available evidence suggests that valerian might improve sleep quality without producing side effects"⁴.

Disruptions in sleep and circadian rhythm have been shown to be associated with elevated breast cancer risk^{5,6}. The International Agency for Research on Cancer (IARC) has designated circadian disruption caused by night shift work as a "2A" carcinogen (probably carcinogenic) for breast cancer^{7,8}. This designation is reaffirmed by the finding of a 40% elevated risk of breast cancer risk among female night shift workers in a recent meta-analysis⁶. In breast tumors, many human circadian genes have been found to be dysregulated⁹. Animal studies have also demonstrated that mice with disruptions in their molecular clocks showed increased breast cancer risk¹⁰ and accelerated growth rates of malignant tumors¹¹.

Given the connection between circadian factors and tumorigenesis, the herb's ability to ameliorate sleep dysfunction may signify a completely unexplored underlying anti-tumorigenic capacity. Valeric acid, a short

¹Department of Environmental Health Sciences, Yale University School of Public Health, New Haven, CT 06520, USA. ²Department of Oncology and Hematology, Dongzhimen Hospital, Beijing University of Chinese Medicine, Beijing 100700, China. ✉email: yong.zhu@yale.edu

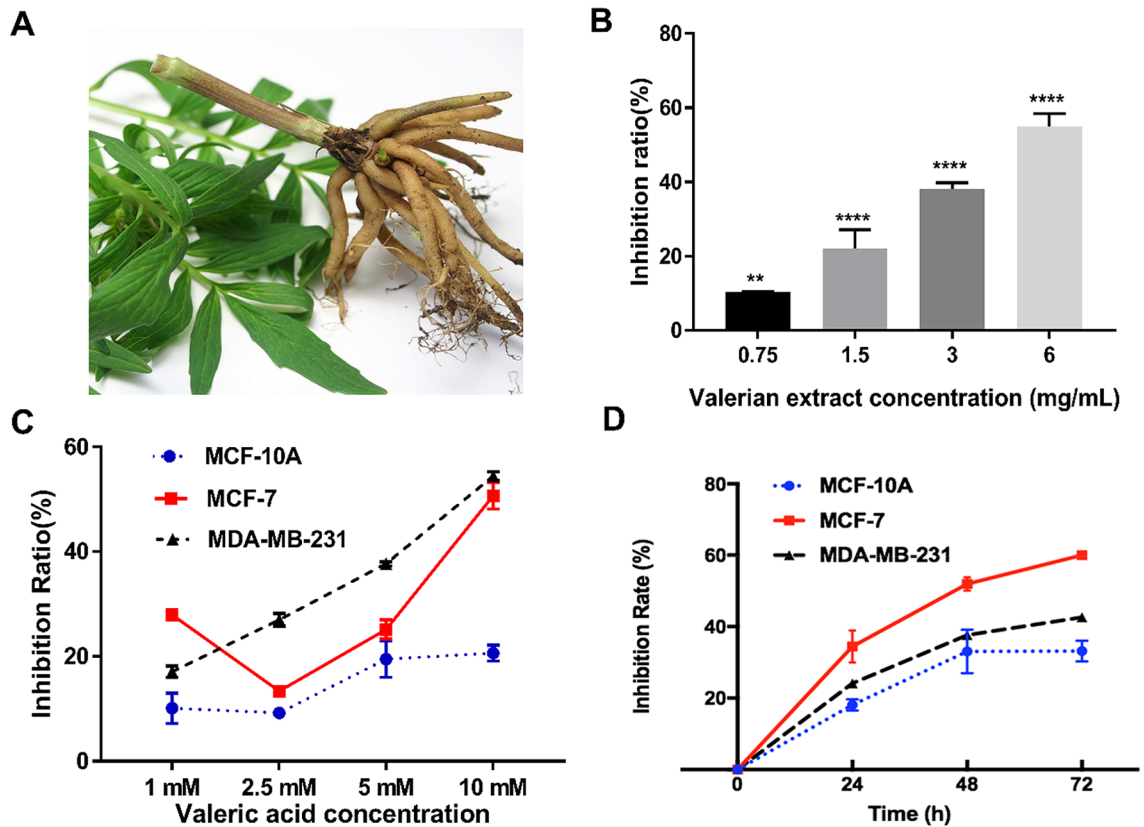


Figure 1. Cell proliferation inhibitory effect of valerian extract and valeric acid on breast cancer cells. (A) A picture of Valerian root. (B) Valerian inhibited the growth of MCF-7 cells in a dose-dependent manner. MCF-7 cells were incubated with valerian extract in different concentrations (0.75 mg/mL, 1.5 mg/mL, 3 mg/mL, and 6 mg/mL) and significant inhibition of cell proliferation was observed after 48 h. (C) Cell proliferation inhibitory effect of valeric acid on MCF-7, MDA-MB-231 and MCF-10A cells at different concentrations (1 mM, 2.5 mM, 5 mM, and 10 mM) and the inhibition of cell proliferation was measured after 48 h. (D) Cell proliferation inhibitory effect of valeric acid on MCF-10A, MDA-MB-231 and MCF-7 cells at 24 h, 48 h, and 72 h. Cells were incubated with 5 mM of valeric acid and all experiments were performed in triplicate.

chain fatty acid (SCFA), is a major active chemical ingredient of valerian and shares a high structural similarity with the known histone deacetylase inhibitor (HDACi) valproic acid^{12–14}. HDACi is a novel group of anti-cancer drugs, which may reverse gene-associated DNA methylation and influence gene expression levels¹⁵. Considering the role of circadian factors in breast cancer tumorigenesis and the potential HDAC inhibiting function, we tested the hypothesis that valeric acid could provide therapeutic benefits against human breast cancer through epigenetic modifications, including DNA methylation and histone deacetylation in the current study.

Results

Valerian and valeric acid reduce proliferation of breast cancer cells. Figure 1A shows a picture of Valerian root. Compared to the control group, cell proliferation rates of valerian treated MCF-7 cells (0.75 mg/mL, 1.5 mg/mL, 3 mg/mL, 6 mg/mL) were significantly inhibited at 48 h by $10.39 \pm 0.12\%$ ($p = 0.0038$), $22.16 \pm 5.02\%$ ($p < 0.001$), $38.22 \pm 1.62\%$ ($p < 0.001$) and $55.01 \pm 3.46\%$ ($p < 0.001$), respectively (Fig. 1B). We then tested anti-proliferative activity of valeric acid at different concentrations against breast cancer cell lines MCF-7, MDA-MB-231 and normal breast epithelial cells MCF-10A at 48 h. Results showed that valeric acid (1 mM, 2.5 mM, 5 mM, and 10 mM) inhibited MCF-7 cells by $27.92 \pm 1.05\%$ ($p = 0.009$), $13.36 \pm 0.60\%$ ($p = 0.037$), $25.15 \pm 1.83\%$ ($p = 0.006$), $50.67 \pm 2.57\%$ ($p = 0.001$), and inhibited MDA-MB-231 cells by $17.07 \pm 1.11\%$ ($p < 0.001$), $26.99 \pm 1.21\%$ ($p < 0.001$), $37.65 \pm 1.35\%$ ($p < 0.001$), $54.44 \pm 0.85\%$ ($p < 0.001$) at 48 h, respectively (Fig. 1C). Valeric acid at 5 mM was further tested for anticancer effect at different time points. Specifically, the proliferation of MCF-7 cells was inhibited by $34.48 \pm 3.64\%$ ($p = 0.007$), $51.95 \pm 2.04\%$ ($p < 0.001$), and $60.02 \pm 0.53\%$ ($p < 0.001$) at 24 h, 48 h, 72 h, respectively, versus $24.13 \pm 0.76\%$ ($p = 0.003$), $37.65 \pm 0.35\%$ ($p < 0.001$), and $42.16 \pm 1.91\%$ ($p = 0.001$) for MDA-MB-231; and $17.01 \pm 0.58\%$ ($p < 0.001$), $33.21 \pm 3.55\%$ ($p = 0.016$), and $33.18 \pm 3.55\%$ ($p = 0.002$) for MCF-10A at the concentration of 5 mM (Fig. 1D). Overall, valeric acid showed strong inhibitory effect on MCF-7 and MDA-MB-231 breast cancer cell lines and relatively less inhibitory effect on the MCF-10A cell line.

Effect of valeric acid on migration of breast cancer cells. A wound healing assay was performed to examine the migration and invasiveness of breast cancer cells treated by valeric acid. For MDA-MB-231 cells, the percentage of wound closure for control, 5 mM and 10 mM groups were $60.48 \pm 2.97\%$, $40.48 \pm 2.18\%$ and

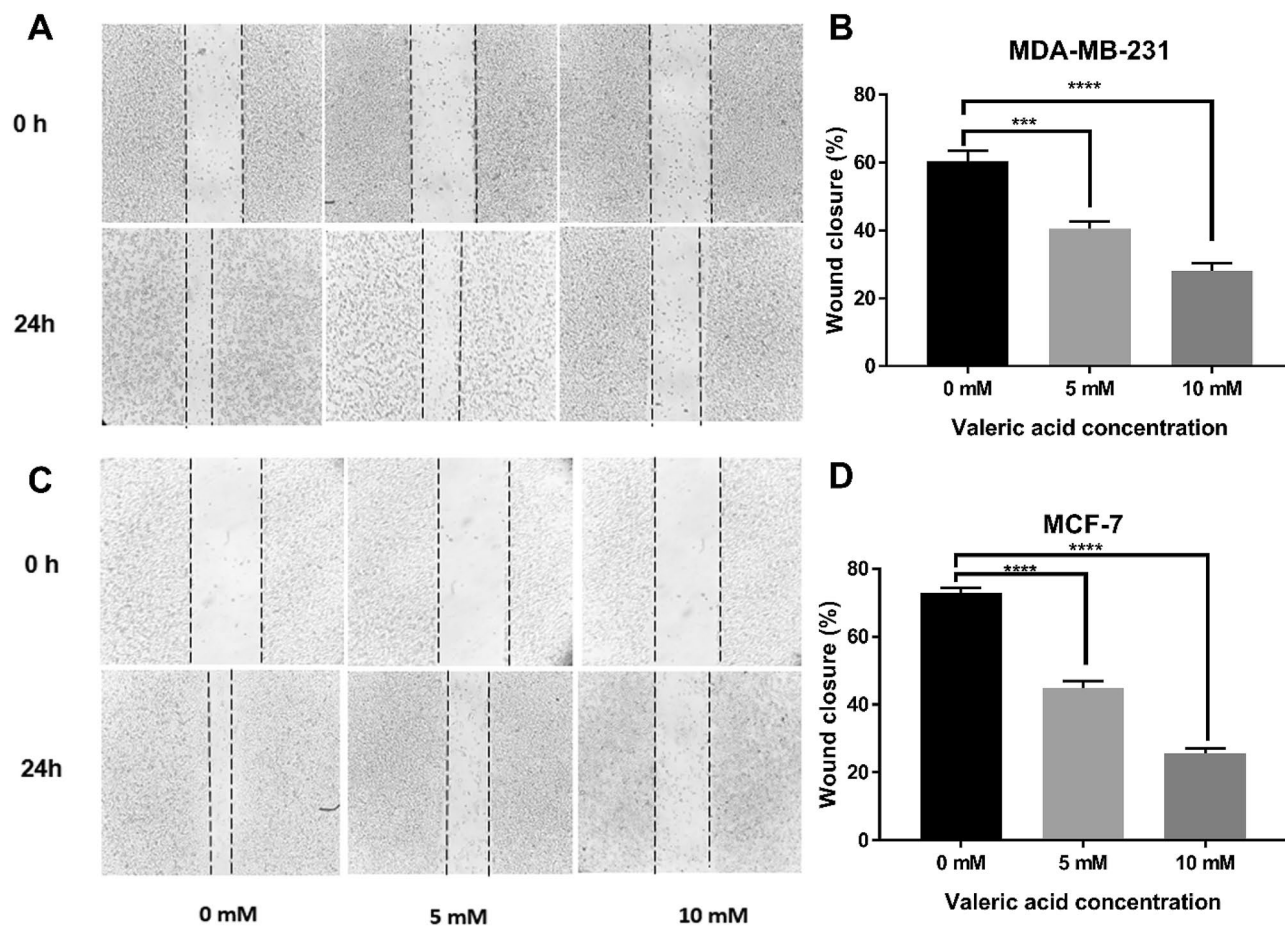


Figure 2. Effect of valeric acid on migration of MCF-7 and MDA-MB-231 cells. Monolayer cells were scraped by a sterile micropipette tip and then treated with various concentrations of valeric acid for 24 h. (A,B) MDA-MB-231 cells migrated to the wounded region were photographed (100× magnification). (C,D) MCF-7 cells migrated to the wounded region were photographed (100× magnification). The wound closure of the cell cultures was presented in the middle field of each treatment, and data were calculated from three independent experiments. All experiments were performed in triplicate.

28.10 ± 2.18% (Fig. 2A,B), and 72.86 ± 1.43%, 44.76 ± 2.18% and 25.71 ± 1.43% for MCF-7 (Fig. 2C,D), respectively, with a significant difference ($p < 0.001$) in all comparisons.

Effect of valeric acid on colony formation of breast cancer cells. The colony formation assay showed reduced cell colony formation ability of the cells (MCF-7 and MDA-MB-231) in valeric acid treated groups (Fig. 3A,B). Figure 3C revealed that the calculated relative colony formation efficiency was 44.84 ± 8.05% for MCF-7 cells treated by valeric acid ($p < 0.001$) and 68.9 ± 10.72% for MDA-MB-231 cells treated by valeric acid ($p < 0.001$).

Inhibition of 3D formation by valeric acid. To investigate the impact of valeric acid on cell 3D condition that mimics breast cancer cell growth in vivo, the relative cross-section area formation efficiency was calculated by the comparison to their original area size (24 h) in each group, respectively. As shown in Fig. 4, for MDA-MB-231 cells, relative cell cross-section area of valeric acid treated group reached to 103.52 ± 2.77% at 48 h, and showed a significant difference compared to its counterparts of the control group (121.34 ± 2.61%, $p < 0.001$). At 96 h, the trend still remained, relative area of valeric acid treated group reached to 168.54 ± 9.67% compared to 180.73 ± 8.86% of the control group ($p = 0.029$). Similarly, a significantly smaller spheroid area was observed in the valeric acid treated group compared to the control at both 48 h and 96 h ($p < 0.001$) in experiment using MCF-7 cells.

Effect of valeric acid on HDAC activity. MCF-7 cells were treated with 2.5 mM, 5 mM, and 10 mM of valeric acid and HDAC activity was measured after 48 h (Fig. 5A). The HDAC activity inhibition ratio of cells treated with 2.5 mM valeric acid was 40.44 ± 1.88% that showed a significant reduction compared to the control group ($p = 0.028$). Similarly, the HDAC activity of MCF-7 cells was inhibited by 53.15 ± 0.68% ($p = 0.002$) at the

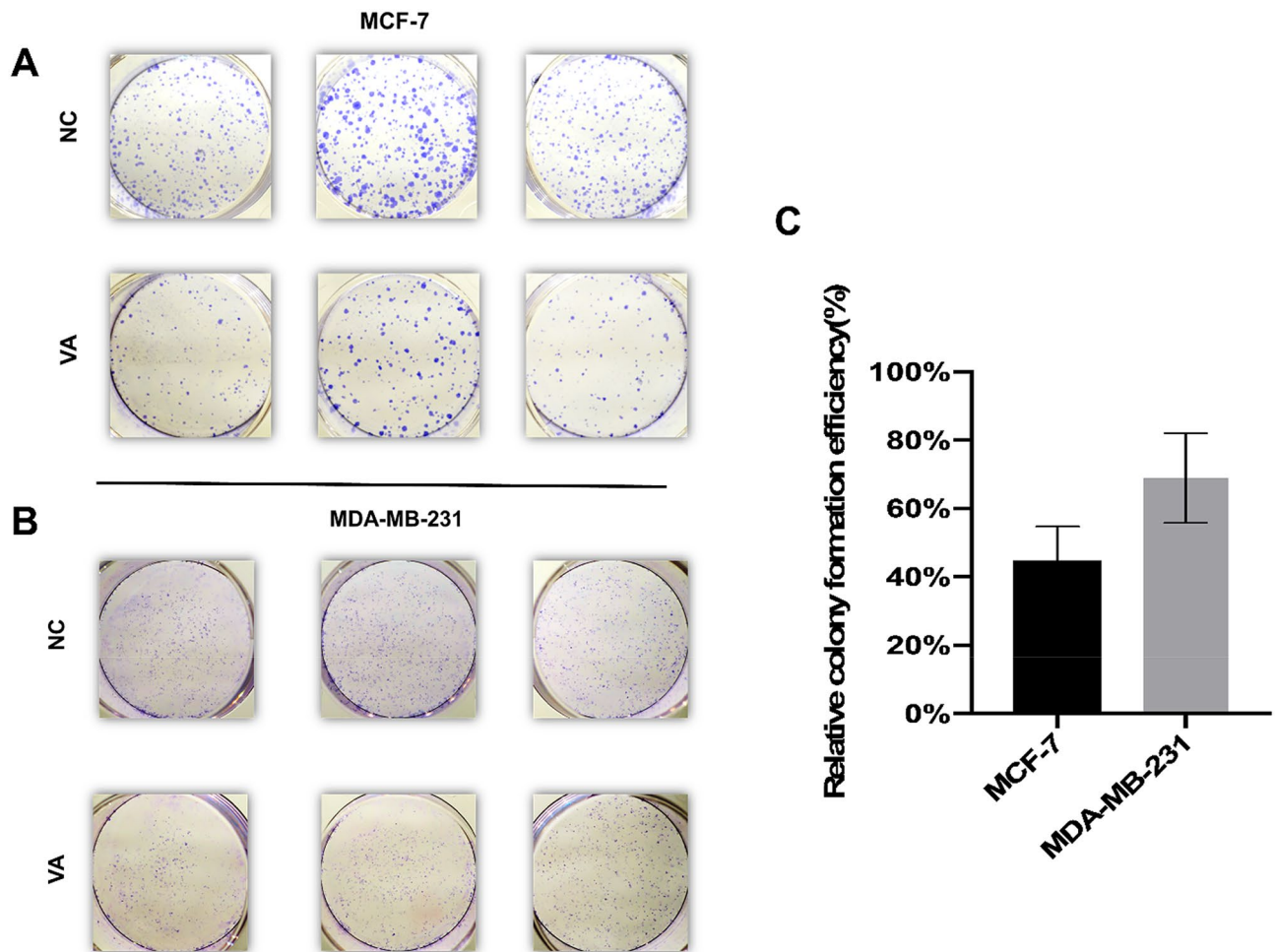


Figure 3. Valeric acid suppresses the colony formation ability of MCF-7 and MDA-MB-231. The representative colony formation of MCF-7 (A) and MDA-MB-231 (B) cells intervened by valeric acid (VA) and PBS, respectively. The relative colony formation efficiency showed reduction in number of colonies of both cells (C). Data are presented as the mean \pm standard deviation (SD).

concentration of 5 mM valeric acid and $61.64 \pm 2.10\%$ ($p < 0.001$) at the concentration of 10 mM valeric acid compared to the control group.

Effect of valeric acid on global DNA methylation. A dose-dependent effect of valeric acid on the global DNA methylation levels in MCF-7 cells was observed. MCF-7 breast cancer cells were incubated with 2.5 mM, 5 mM, and 10 mM of valeric acid and global DNA methylation was measured at 72 h. Global DNA methylation levels associated with different concentrations of valeric acid were $0.76 \pm 0.02\%$ ($p < 0.001$), $0.53 \pm 0.04\%$ ($p < 0.001$) and $0.34\% \pm 0.02$ ($p < 0.001$), respectively, versus $1.89 \pm 0.03\%$ for the control group in MCF-7 cells (Fig. 5B), indicating decreased global DNA methylation levels associated with increased valeric acid concentrations.

Epigenetic landscape changes affected by valeric acid. To better understand epigenetic landscape changes affected by valeric acid, we performed the genome-wide DNA methylation assay followed by network-based analysis. Our data showed that 1398 CpG sites were differentially methylated across 1075 unique genes (Supplementary table). Significant CpG sites with methylation differences were determined by adjusted p values (FDR $p < 0.05$). Delta-beta ranges from -0.14 to -0.52 for hypomethylated sites and from 0.14 to 0.83 for hypermethylated sites. Of these sites, 1267 CpG sites were hypermethylated while 131 CpG sites were hypomethylated in treated cells. According to the reference location of the probes used for each CpG site, we found that 229 CpG sites with differential methylation are located in either 5'UTR or 3'UTR regulatory regions. Sixty-three genes have multiple CpG sites with differential methylation and these CpG sites in 57 of these genes are either all hyper- or hypo-methylated.

Among differentially methylated genes, there were 15 histone-related genes including histone deacetylase 6 (HDAC6) that was hypermethylated. The network identified by the IPA tool as being most significantly associated with the set of input genes was designated as having functional relevance in "RNA post-transcriptional modification, cancer, and developmental disorder" ($p = 10^{-59}$) as illustrated in Fig. 6. Briefly, 27 genes were present in

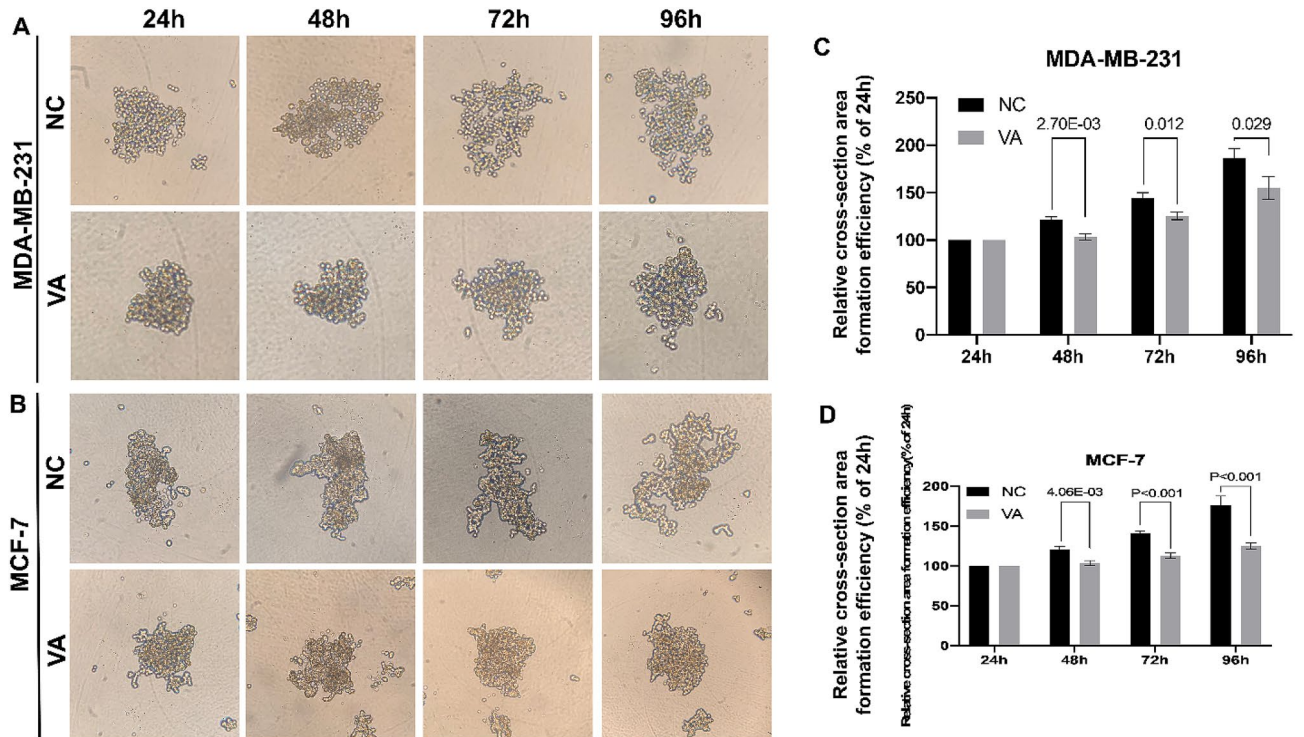


Figure 4. Valeric acid inhibits the 3D formation of MCF-7 and MDA-MB-231 cells. (A) illustrated the dynamic changes of 3D formation for MDA-MB-231 cells. (B) showed the dynamic changes of 3D formation for MCF-7 cells. Their relative cross-section area formation efficiencies were shown in (C,D). Significant reduction of cross-section area of MDA-MB-231 cells (C) and MCF-7 cells (D) in VA treated groups were observed.

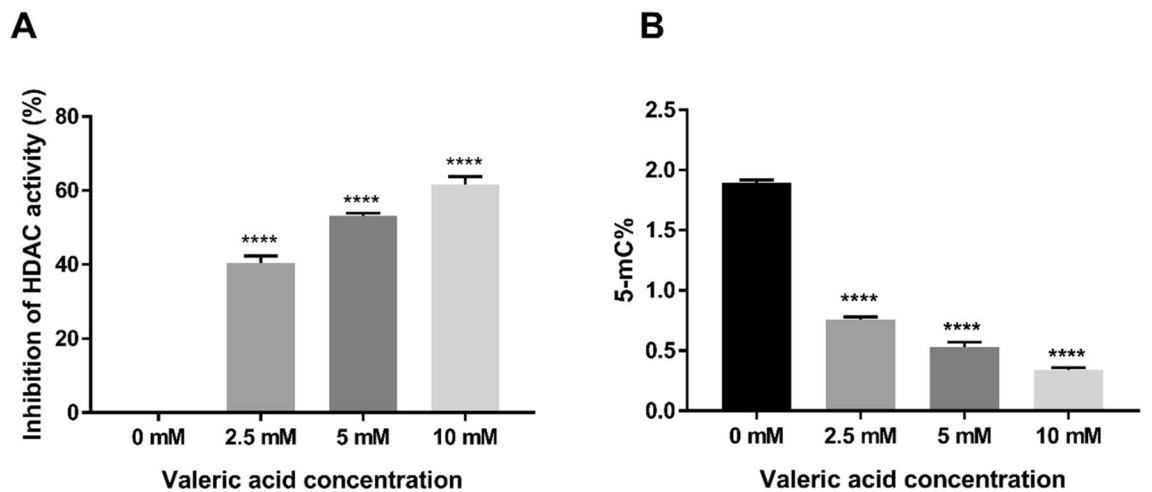


Figure 5. Impact of valeric acid on HDAC activity and global DNA methylation. (A) MCF-7 cells were incubated at three different concentrations of valeric acid and HDAC activity was measured after 48 h. Valeric acid significantly inhibited HDAC activity at concentration of 2.5 mM, 5 mM, and 10 mM compared to the control group ($*p < 0.05$). (B) The Global DNA methylation assay revealed that valeric acid (2.5 mM, 5 mM, and 10 mM) significantly decreased the levels of global DNA methylation in MCF-7 cells compared to the control group ($*p < 0.05$). All assays were performed in triplicate.

the network, 26 of which were significantly hypermethylated, while 1 of which was hypomethylated in treated cells. Several putative tumor related genes with oncogenic role in breast cancer were hypermethylated, such as *HDAC6*, *NASP*, *HNRNPC* and *LIN9*.

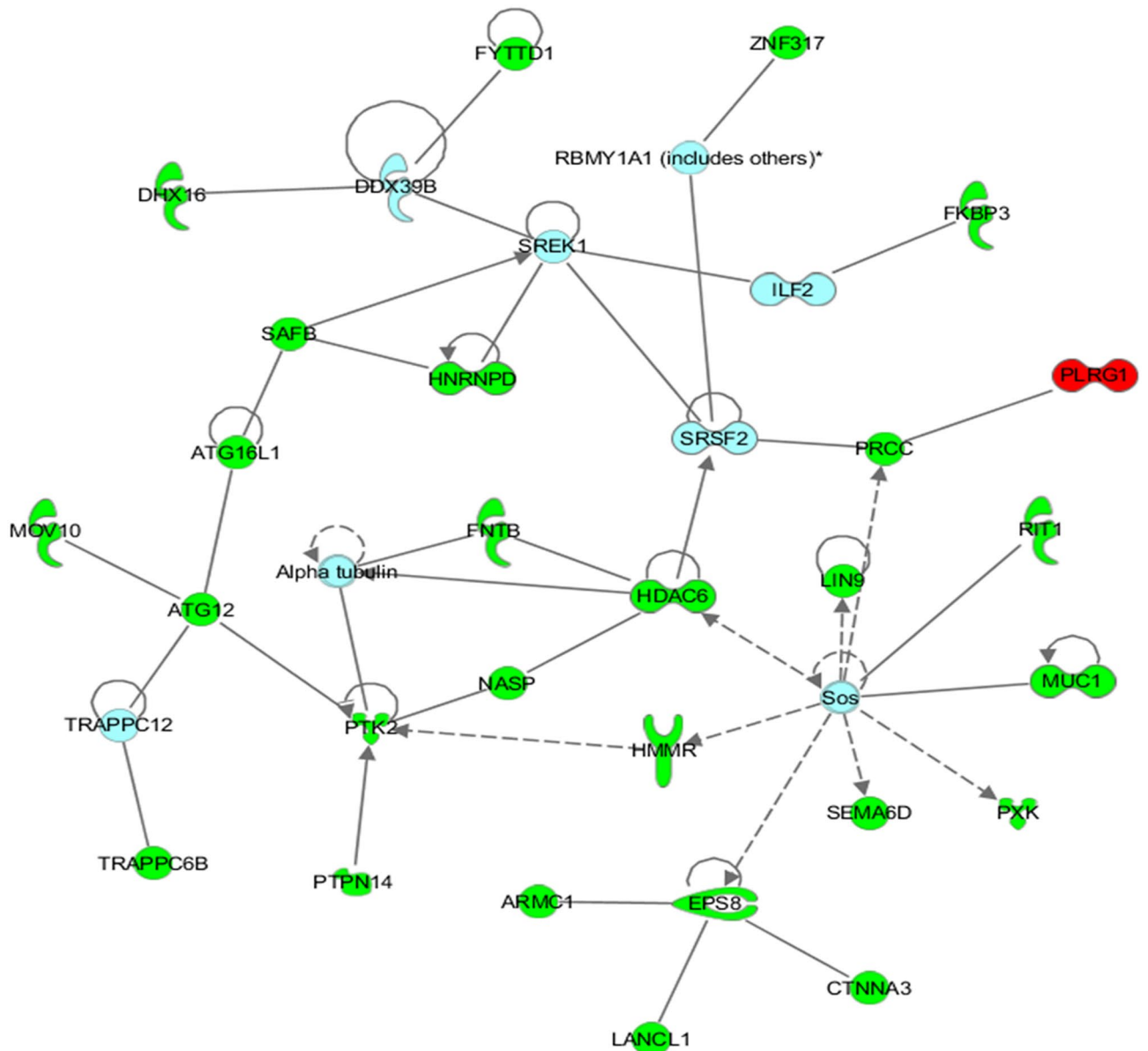


Figure 6. Network of interactions significantly enriched for genes displaying altered methylation patterns following treatment with valeric acid. This network was identified by the IPA as being the most significantly associated with the set of input genes and molecules within this network have functional relevance in “RNA post-transcriptional modification, Cancer, and Developmental disorder” ($p = 10E-59$). Of the 27 genes present in the network, 26 were significantly hypermethylated and are shaded in green, while only 1 was hypomethylated and shaded in red. Each interaction is supported by at least one literature reference identified in the Ingenuity Pathway Knowledge Base, with solid lines representing direct interactions, and dashed lines representing indirect interactions.

Discussion

Despite being the most commonly used herb (or herbal remedy) for sleep disorders, the efficacy of valerian root to treat cancer remained unexplored. We have shown that valerian root and valeric acid (a major compound of valerian root) can inhibit proliferation, migration, colony formation and 3D formation of breast cancer cells in a dose- and time-dependent manner. Moreover, this inhibitory effect was significantly decreased on normal breast epithelial cells compared to breast cancer cells, indicating a cancer-specific action with low side-effects. These findings support our hypothesis that the sleep-related herb, valerian root, may provide therapeutic benefits against human breast cancer.

To explore the underlying basis of the functional effect of valeric acid, we also conducted the HDAC activity assay because valeric acid shares a high structural similarity with the known histone deacetylase inhibitor (HDACi) valproic acid^{12–14}. Histone acetylation is an important epigenetic modification and HDAC inhibitors are among the most promising targets in the development of drugs for cancer therapy¹⁶. More than 15 HDAC

inhibitors have been tested in preclinical and clinical studies. Inhibition of HDAC leads to the acetylation of non-histone proteins such as tumor suppressor p53¹⁷, which may exhibit antiproliferative properties^{18,19}. Our data demonstrate that valeric acid significantly decreases HDAC activity in treated breast cancer cells, which provides a possible mechanism to account for its anticancer efficacy. This result suggests that valeric acid may serve as a novel HDACi for breast cancer chemotherapy.

Histone acetylation may modify chromatin and most DNA methylation related proteins (DNA methyltransferase Dnmt1, several methyl-CpG binding proteins, MeCP2, MBD2, and MBD3) are associated with histone deacetylase²⁰. These enzymes regulate the process of DNA methylation¹⁵ and the HDAC activity reduced by valeric acid treatment may lead to alterations of DNA methylation. Our results support this assertion by showing that both global DNA methylation level and gene specific DNA methylation status were affected by valeric acid. Of particular interest, genome-wide DNA methylation screening detected 15 histone-related genes, including histone deacetylase 6 (HDAC6), to be hypermethylated, which is in congruent with the observed decreased HDAC activity in valeric acid treated cancer cells.

Hypermethylated HDAC6 gene may have anticancer properties because HDAC6 was significantly overexpressed in, not only breast cancer²¹, but also various other tumor types²². Histone deacetylase 6 (HDAC6) is a unique member of the HDAC family and plays an important role in regulating the function of HSP90, α -tubulin, and the aggresome²³ and effects on functional reduction of these downstream oncogenic targets may account for the growth inhibitory effects of HDAC6 knockdown.

We also searched for transcription factor binding sites in the scouse sequence (50 bases) of HDAC6 5'UTR that harbors the hypermethylated CpG site using the PROMO tool²⁴ and identified binding sites of 4 transcription factors, Pax-5 (GGGCCTG/CCTGCCC), p53 (CCTGCCC), AP-2 alphaA (GCCTGC), and C/EBP beta (GCAA). All of these 4 transcription factors have been shown to play roles in breast tumorigenesis^{25–28}, which warrants further investigation on molecular mechanisms of valeric acid efficacy.

In addition to HDAC6, several other putative tumor related genes with oncogenic role in breast cancer were hypermethylated after valeric acid treatment in our study. NASP, nuclear autoantigenic sperm protein, has become an important constituent of “poor prognosis signature” in breast cancer patients²⁹. Depletion of the histone chaperone tNASP inhibits proliferation and induces apoptosis in prostate cancer PC-3 cells³⁰ and human gastric cancer³¹. HNRNPC, heterogeneous nuclear ribonucleoproteins C, is a RNA binding protein and its elevated expression has been reported in cancer cells³², but the function of HNRNPC in tumors is still not clear. Repression of HNRNPC in breast cancer cells MCF7 and T47D was reported to inhibit cell proliferation and tumor growth³³. LIN9 is a part of the MuvB core complex (composed of LIN9, LIN52, LIN37, LIN54, and RBBP4), which functions as a transcriptional regulator of mitosis. Overexpression of LIN9 has been observed in the majority of triple-negative breast cancers (TNBCs) and is associated with poor prognosis across breast cancer subtypes³⁴. Hypermethylation of these putative oncogenes may provide a new mechanism accounting for the observed anticancer efficacy of valeric acid in addition to the HDAC mediated processes.

Changes or alterations in both histone acetylation and DNA methylation are common targets studied in cancer epigenomics because these epigenetic processes are generally involved in cell proliferation, differentiation, and survival, and are linked to carcinoma progression^{35,36}. Discovering chemicals that can modify these epigenetic processes is a promising new strategy for drug development in cancer chemotherapy. The functional effects of valeric acid in the inhibition of histone deacetylase and alteration of DNA methylation make it a promising novel epigenetic agent for future clinical implications in breast cancer treatment.

Although a profound anticancer effect is observed, findings from this study are still preliminary, which need to be further confirmed in more breast cancer cell lines and animal models. More mechanistic studies are also necessary to further evaluate other epigenetic effects of valeric acid. Inhibition rates of valeric acid on MCF-7 cells (not MDA-MB-231) decrease at low concentrations and then increase again at high doses in cell proliferation assay. This might be due to hormone receptor status of these 2 cells. MCF-7 is a breast cancer cell line with estrogen, progesterone and glucocorticoid receptors and MDA-MB-231 is a triple negative breast cancer cell line. Agents such as valeric acid may have different types of dose-responses (i.e. bell-shaped and U-shaped dose–response curves) when used to treat different tumor types. More breast cancer cell lines and doses are needed to confirm this observation in future study. Nonetheless, as the promising profile of valeric acid were well established, valeric acid is a potential new therapeutic agent for breast cancer and probably cancer in general, worthy of further investigation.

Materials and methods

Cell lines and cell culture. Human breast cancer cells MCF-7 and MDA-MB-231, and normal breast epithelial cells MCF-10A were purchased from the American Type Culture Collection (ATCC) (Manassas, VA, USA). MCF-10A cells were maintained in MEGM (Life Technologies, CA, USA) supplemented with 100 ng/mL cholera toxin. MCF-7 and MDA-MB-231 cells were cultured in DMEM (Life Technologies, CA, USA) supplemented with 10% fetal bovine serum, 1% penicillin–streptomycin. The cells were cultured at 37 °C in a humidified atmosphere consisting of 5% CO₂. The culture medium was changed once every 2 days.

Preparation of valerian extract and valeric acid. Valerian and valeric acid were purchased from Chromadex (Irvine, CA, USA). Valerian was received as a powder from the herb pulverized rhizome. To prepare the extract of valerian for experiments, 250 mg of this powder was diluted in 2 mL of distilled water, heated to 100 °C for 20 min in a water bath and centrifuged at 1000g for 10 min. The supernatant was filtered through a hydrophilic membrane containing 0.22 μ M pores (Millipore, Billerica, MA, USA). Valeric acid was diluted in culture medium to obtain working concentrations.

Cell proliferation assay. We first tested the anticancer effect of valerian on the growth of breast cancer cells using cell proliferation assay. MCF-7 cells were harvested and seeded into each well of 96-well plates at the concentration of 4000 cells/100 μ L, and different concentrations of valerian extract (0.75 mg/mL, 1.5 mg/mL, 3 mg/mL, and 6 mg/mL, final concentrations after dilution with medium) or the same volume of ddH₂O (control group) were added to each well. After incubation for 48 h, we added 20 μ L of MTS assay (Promega, Wisconsin, USA) per well in a dark hood and then incubated plates for 2 h. Optical density (OD) was determined at the wavelength of 490 nm by a microplate Spectrophotometer (Biotek, Winooski, USA). MCF-7, MDA-MB-231 and MCF-10A cell lines were used to detect the efficacy of valeric acid on the proliferation of breast cancer cells. Cells were seeded into 96-well plates as described above. 1 mM, 2.5 mM, 5 mM, and 10 mM of valeric acid or the same volume of ddH₂O were added and OD values were measured at different time points. Triplicate were conducted for each condition at each time point. The proliferation inhibition rate was calculated using the formula as: inhibition ratio = $(1 - OD_{\text{treated group}}/OD_{\text{control group}}) \times 100\%$. The inhibition ratio was fitted to a non-linear regression plot to determine the IC₅₀ (half maximal inhibitory concentration) for breast cancer cells treated with valerian extract or valeric acid.

Wound-healing assay. In order to understand how valeric acid affects cancer cell migration and confirm the cell proliferation results, we performed a wound-healing assay. Approximately 1×10^6 MCF-7 or MDA-MB-231 cells were added into each well of 6-well tissue culture plates with culture medium containing 10% FBS and grew to nearly 80–90% confluence. A scratch was gently made using a 100 μ L pipette tip in each well and the cells were washed with PBS twice to remove the detached cells. Cells were then treated with different concentrations of valeric acid or the same amount of ddH₂O with 0.1% FBS at 37 °C for 24 h. Wound-healing assay was conducted in triplicate. Images were taken at 0 h and 24 h and the area of a wound was measured with ImageJ software (version of 1.52a) and the average extent of wound closure was quantified.

Colony formation assay. To examine relatively long-time (~10 days) inhibitory impact of valeric acid on the growth of breast cancer cells, we conducted a colony formation assay. Approximately 3000 MCF-7 or MDA-MB-231 cells were seeded into 6-well tissue culture plates with 2 mL complete medium per well. Cells were treated with 0.85 mM valeric acid or the same amount of ddH₂O (control group). Cells were cultured for 10 days and drug-containing culture medium was renewed once every 3 days. Cells were then fixed by 4% paraformaldehyde (FD NeuroTechnologies, USA) and dyed with 0.05% crystal violet (Sigma-Aldrich, USA) at room temperature. Images were taken and the number of colonies with more than 50 cells was counted manually. Relative colony formation efficiency = (amount of colony in treated group/amount of colony in control group) \times 100%.

3D formation assay. We simulated in vivo cancer cell survival when treated with valeric acid by performing a 3D formation assay. A hanging drop method has been successfully developed for generation of 3D spheroids that enables the growth of cells in a multidimensional and multicellular manner and facilitates cancer study and more efficient drug screening^{37,38}. Briefly, MDA-MB-231 or MCF-7 cells were placed into each drop which contained 20 μ L complete medium and 200 cells, respectively. 0.85 mM valeric acid or the same amount of ddH₂O (control group) was then added into each drop. All drops were cultured in a humidified incubator at 37 °C with 5% CO₂. Images were taken at different time points (24 h, 48 h, 72 h, 96 h). The cross-section area of 3D spherical formation was calculated by software ImageJ (version of 1.52a).

HDAC colorimetric activity assay. The effect of valeric acid on histone deacetylase (HDAC) activity was assessed using the Colorimetric HDAC Activity Assay Kit (BioVison, Milpitas, CA, USA) according to the manufacturer's instructions. Briefly, MCF-7 cells were treated with various concentrations of valeric acid for 48 h, at which point nuclear protein fractions were prepared using the Epiquik Nuclear Extraction Kit (Epigentek, USA) following the manufacturer's protocols. 50 μ g of nuclear extracts from treated cells were then diluted in 85 μ L ddH₂O. 10 μ L of 10 \times HDAC assay buffer was added followed by the addition of 5 μ L of the colorimetric substrate. Samples were then incubated at 37 °C for 1 h. Subsequently, the reaction was stopped by adding 10 μ L of lysine developer and left for an additional 30 min at 37 °C. OD values of samples were read by microplate spectrophotometer (Biotek, Winooski, USA) at the wavelength of 405 nm. HDAC activity was expressed as relative OD values per μ g of protein sample. The assay was conducted in triplicate.

Global DNA methylation assay. MCF-7 cells were treated with 5 mM valeric acid for 72 h and then collected for genomic DNA isolation using the QIAamp DNA Blood Mini Kit (Qiagen Sciences, Maryland, MD, USA). The Global DNA methylation levels were determined using the MethylFlash Global DNA Methylation Quantification Kit (Epigentek, NY, USA) according to the manufacturer's instructions. The absorbance of the samples was measured on microplate reader at 450 nm. The experiment was performed in triplicate. For the OD intensity to be proportional to the amount of methylated DNA, the % 5-mC was calculated using the following formula: 5-mC% = $[(\text{sample OD} - \text{negative control OD}) \times P / (\text{positive control OD} - \text{negative control OD}) \times S \times 2] \times 100\%$, where S represents the amount of input sample DNA (100 ng) and P represents the amount of input positive control DNA (5 ng).

Genome-wide DNA methylation array. To further explore epigenetic impact of valeric acid on specific CpG sites in cancer related genes, we performed a genome-wide DNA methylation analysis. Genomic DNA of MCF-7 cells treated with 5 mM valeric acid for 72 h was isolated and purified using the QIAamp DNA Blood Mini Kit (Qiagen Sciences, Maryland, MD, USA) according to the manufacturer's protocols. 50 ng of genomic

DNA per sample was used for the analysis using the Infinium Human Methylation 450 BeadChips (Illumina, San Diego, CA USA). A methylation index (β) was used to estimate the methylation level of each CpG site using the ratio of intensities between methylated and unmethylated cytosines, which is a continuous variable between 0 and 1. 0 corresponds to a completely unmethylated site, while 1 corresponds to a completely methylated site. Significant methylation differences in methylation levels between treated and control group at each CpG site were obtained using The Illumina Custom Model.

Network analysis. The Ingenuity Pathway Analysis software (IPA, Ingenuity Systems) (Redwood City, CA) was used to investigate whether differentially methylated genes were enriched for functional relationships between treated and control groups. Differentially methylated genes were input into the program and used to identify experimentally verified interactions using the Ingenuity Knowledge Base, a manually curated database of functional interactions extracted from peer reviewed publications³⁹. *p* values for individual networks were obtained by comparing the likelihood of obtaining the same number of genes or greater in a random gene set as are actually present in the input set using a Fisher's exact test, based on the hypergeometric distribution.

Statistical analysis. All statistics and figures were generated using the GraphPad Prism 7.00 software (www.graphpad.com) if not specified. All results were shown as mean \pm standard error. All *p* values presented were two-sided and *p* < 0.05 was regarded as statistically significant.

Ethical approval. This article does not contain animal studies and any studies with human participants performed by any of the authors.

Received: 28 September 2020; Accepted: 6 January 2021

Published online: 28 January 2021

References

- Cragg, G. M. & Newman, D. J. Plants as a source of anti-cancer agents. *J. Ethnopharmacol.* **100**, 72–79 (2005).
- Foa, R., Norton, L. & Seidman, A. D. Taxol (paclitaxel): a novel anti-microtubule agent with remarkable anti-neoplastic activity. *Int. J. Clin. Lab. Res.* **24**, 6–14 (1994).
- Block, K. I., Gyllenhaal, C. & Mead, M. N. Safety and efficacy of herbal sedatives in cancer care. *Integr. Cancer Ther.* **3**, 128–148. <https://doi.org/10.1177/1534735404265003> (2004).
- Bent, S., Padula, A., Moore, D., Patterson, M. & Mehling, W. Valerian for sleep: a systematic review and meta-analysis. *Am. J. Med.* **119**, 1005–1012. <https://doi.org/10.1016/j.amjmed.2006.02.026> (2006).
- Viswanathan, A. N. & Schernhammer, E. S. Circulating melatonin and the risk of breast and endometrial cancer in women. *Cancer Lett.* **281**, 1–7 (2009).
- Samuelsson, L. B., Bovbjerg, D. H., Roecklein, K. A. & Hall, M. H. Sleep and circadian disruption and incident breast cancer risk: an evidence-based and theoretical review. *Neurosci. Biobehav. Rev.* **84**, 35–48. <https://doi.org/10.1016/j.neubiorev.2017.10.011> (2018).
- Straif, K. *et al.* Carcinogenicity of shift-work, painting, and fire-fighting. *Lancet Oncol.* **8**, 1065–1066 (2007).
- Group, I. M. V. Carcinogenicity of night shift work. *Lancet Oncol.* **20**, 1058–1059. [https://doi.org/10.1016/S1470-2045\(19\)30455-3](https://doi.org/10.1016/S1470-2045(19)30455-3) (2019).
- Chen, S. T. *et al.* Deregulated expression of the PER1, PER2 and PER3 genes in breast cancers. *Carcinogenesis* **26**, 1241–1246 (2005).
- Sahar, S. & Sassone-Corsi, P. Circadian clock and breast cancer: a molecular link. *Cell Cycle* **6**, 1329–1331 (2007).
- Filipinski, E. *et al.* Host circadian clock as a control point in tumor progression. *J. Natl. Cancer Inst.* **94**, 690–697 (2002).
- Gurvich, N., Tsygankova, O. M., Meinkoth, J. L. & Klein, P. S. Histone deacetylase is a target of valproic acid-mediated cellular differentiation. *Cancer Res.* **64**, 1079–1086. <https://doi.org/10.1158/0008-5472.can-03-0799> (2004).
- Fuks, F., Burgers, W. A., Brehm, A., Hughes-Davies, L. & Kouzarides, T. DNA methyltransferase Dnmt1 associates with histone deacetylase activity. *Nat. Genet.* **24**, 88–91 (2000).
- Fuks, F., Hurd, P. J., Deplus, R. & Kouzarides, T. The DNA methyltransferases associate with HP1 and the SUV39H1 histone methyltransferase. *Nucleic Acids Res.* **31**, 2305–2312 (2003).
- Sarkar, S. *et al.* Histone deacetylase inhibitors reverse CpG methylation by regulating DNMT1 through ERK signaling. *Anticancer Res.* **31**, 2723–2732 (2011).
- Suraweera, A., O'Byrne, K. J. & Richard, D. J. Combination therapy with histone deacetylase inhibitors (HDACi) for the treatment of cancer: achieving the full therapeutic potential of HDACi. *Front. Oncol.* **8**, 92. <https://doi.org/10.3389/fonc.2018.00092> (2018).
- Gu, W. & Roeder, R. G. Activation of p53 sequence-specific DNA binding by acetylation of the p53 C-terminal domain. *Cell* **90**, 595–606. [https://doi.org/10.1016/S0092-8674\(00\)80521-8](https://doi.org/10.1016/S0092-8674(00)80521-8) (1997).
- p21WAF1 is required for butyrate-mediated growth inhibition of human colon cancer cells.
- Joung, K. E., Kim, D. K. & Sheen, Y. Y. Antiproliferative effect of trichostatin A and HC-toxin in T47D human breast cancer cells. *Arch. Pharm. Res.* **27**, 640–645. <https://doi.org/10.1007/Bf02980164> (2004).
- El-Osta, A. & Wolffe, A. P. DNA methylation and histone deacetylation in the control of gene expression: basic biochemistry to human development and disease. *Gene Expr.* **9**, 63–75 (2000).
- Lee, Y. S. *et al.* The cytoplasmic deacetylase HDAC6 is required for efficient oncogenic tumorigenesis. *Can. Res.* **68**, 7561–7569. <https://doi.org/10.1159/0008-5472.Can-08-0188> (2008).
- Yang, W. M., Yao, Y. L., Sun, J. M., Davie, J. R. & Seto, E. Isolation and characterization of cDNAs corresponding to an additional member of the human histone deacetylase gene family. *J. Biol. Chem.* **272**, 28001–28007. <https://doi.org/10.1074/jbc.272.44.28001> (1997).
- Boyault, C., Sadoul, K., Pabion, M. & Khochbin, S. HDAC6, at the crossroads between cytoskeleton and cell signaling by acetylation and ubiquitination. *Oncogene* **26**, 5468–5476. <https://doi.org/10.1038/Sj.Onc.1210614> (2007).
- Messeguer, X. *et al.* PROMO: detection of known transcription regulatory elements using species-tailored searches. *Bioinformatics* **18**, 333–334. <https://doi.org/10.1093/bioinformatics/18.2.333> (2002).
- Kaur, R. P., Vasudeva, K., Kumar, R. & Munshi, A. Role of p53 gene in breast cancer: focus on mutation spectrum and therapeutic strategies. *Curr. Pharm. Des.* **24**, 3566–3575. <https://doi.org/10.2174/1381612824666180926095709> (2018).

26. Turner, B. C. *et al.* Expression of AP-2 transcription factors in human breast cancer correlates with the regulation of multiple growth factor signalling pathways. *Cancer Res.* **58**, 5466–5472 (1998).
27. Zahnow, C. A. CCAAT/enhancer-binding protein beta: its role in breast cancer and associations with receptor tyrosine kinases. *Expert Rev. Mol. Med.* **11**, e12. <https://doi.org/10.1017/S1462399409001033> (2009).
28. Benzina, S. *et al.* Pax-5 is a potent regulator of E-cadherin and breast cancer malignant processes. *Oncotarget* **8**, 12052–12066. <https://doi.org/10.18632/oncotarget.14511> (2017).
29. Martin, K. J., Patrick, D. R., Bissell, M. J. & Fournier, M. V. Prognostic breast cancer signature identified from 3D culture model accurately predicts clinical outcome across independent datasets. *PLoS ONE* **3**, e2994. <https://doi.org/10.1371/journal.pone.0002994> (2008).
30. Alekseev, O. M., Richardson, R. T., Tsuruta, J. K. & O’Rand, M. G. Depletion of the histone chaperone tNASP inhibits proliferation and induces apoptosis in prostate cancer PC-3 cells. *Reprod. Biol. Endocrinol.* **9**, 50. <https://doi.org/10.1186/1477-7827-9-50> (2011).
31. Yu, B. *et al.* microRNA-29c inhibits cell proliferation by targeting NASP in human gastric cancer. *BMC Cancer* **17**, 109. <https://doi.org/10.1186/s12885-017-3096-9> (2017).
32. Park, Y. M. *et al.* Heterogeneous nuclear ribonucleoprotein C1/C2 controls the metastatic potential of glioblastoma by regulating PDCD4. *Mol. Cell. Biol.* **32**, 4237–4244. <https://doi.org/10.1128/MCB.00443-12> (2012).
33. Wu, Y. *et al.* Function of HNRNPC in breast cancer cells by controlling the dsRNA-induced interferon response. *EMBO J.* <https://doi.org/10.15252/emboj.201899017> (2018).
34. Sahni, J. M. *et al.* Mitotic vulnerability in triple-negative breast cancer associated with LIN9 Is targetable with BET inhibitors. *Cancer Res.* **77**, 5395–5408. <https://doi.org/10.1158/0008-5472.CAN-17-1571> (2017).
35. Hecceg, Z. Epigenetics and cancer: towards an evaluation of the impact of environmental and dietary factors. *Mutagenesis* **22**, 91–103. <https://doi.org/10.1093/Mutage/Ge1068> (2007).
36. Esteller, M. Cancer epigenomics: DNA methylomes and histone-modification maps. *Nat. Rev. Genet.* **8**, 286–298. <https://doi.org/10.1038/Nrg2005> (2007).
37. Hao, R. *et al.* A microfabricated 96-well 3D assay enabling high-throughput quantification of cellular invasion capabilities. *Sci. Rep.* **7**, 43390. <https://doi.org/10.1038/srep43390> (2017).
38. Foty, R. A simple hanging drop cell culture protocol for generation of 3D spheroids. *J. Vis. Exp.* <https://doi.org/10.3791/2720> (2011).
39. Calvano, S. E. *et al.* A network-based analysis of systemic inflammation in humans. *Nature* **437**, 1032–1037. <https://doi.org/10.1038/Nature03985> (2005).

Author contributions

Y.Z.: Conception and design. F.S., Y.L., R.H., A.F., R.W., Q.Q.: Development of methodology. F.S., Q.Q.: Acquisition of data. F.S., O.N., Y.Z.: Analysis and interpretation. F.S., O.N., L.H., X.C., Y.Z.: Writing, review, and/or revision of the manuscript. Y.Z.: Administrative, technical, or material support. Y.Z.: Study supervision.

Funding

This work was supported by funds from Yale University and NIH research Grant CA238100. Fengqin Shi, Ya Li, Rui Han and Ronghua Wang were supported by China Scholarship Council (CSC).

Competing interests

The authors declare no competing interests.

Additional information

Supplementary Information The online version contains supplementary material available at <https://doi.org/10.1038/s41598-021-81620-x>.

Correspondence and requests for materials should be addressed to Y.Z.

Reprints and permissions information is available at www.nature.com/reprints.

Publisher’s note Springer Nature remains neutral with regard to jurisdictional claims in published maps and institutional affiliations.



Open Access This article is licensed under a Creative Commons Attribution 4.0 International License, which permits use, sharing, adaptation, distribution and reproduction in any medium or format, as long as you give appropriate credit to the original author(s) and the source, provide a link to the Creative Commons licence, and indicate if changes were made. The images or other third party material in this article are included in the article’s Creative Commons licence, unless indicated otherwise in a credit line to the material. If material is not included in the article’s Creative Commons licence and your intended use is not permitted by statutory regulation or exceeds the permitted use, you will need to obtain permission directly from the copyright holder. To view a copy of this licence, visit <http://creativecommons.org/licenses/by/4.0/>.

© The Author(s) 2021